Possibility of constructing a multispeed Bhatnagar-Gross-Krook thermal model of the lattice Boltzmann method

Minoru Watari*
Wind Tunnel Technology Center, Japan Aerospace Exploration Agency, 7-44-1 Jindaiji Higashi, Chofu, Tokyo 182-8522, Japan

Michihisa Tsutahara
Graduate School of Science and Technology, Kobe University, 1-1 Rokkodai, Nada, Kobe 657-8501, Japan
(Received 12 June 2003; published 15 July 2004)

Multispeed thermal models of the lattice Boltzmann method (LBM) that have a single relaxation [Bhatnagar-Gross-Krook (BGK)] scheme have been proposed by several authors. While these models are intended to correctly represent heat characteristics and compressibility, most of them do not provide satisfactory accuracy. This paper discusses how to construct a correct model. Thermally correct two-dimensional and three-dimensional multispeed LBM BGK models are proposed. The models are verified by simulations of Couette flow, evolution from circularly distributed temperature, and normal shock wave. The results show exact agreement with the theoretical predictions. The numerical stability of the model is demonstrated by the simulation of recovery from a random fluctuation.

DOI: 10.1103/PhysRevE.70.016703 PACS number(s): 47.11.+j, 51.10.+y

I. INTRODUCTION

In the lattice Boltzmann method (LBM), there are two ways of handling thermal fluids. One is the so-called "multicomponent thermal model" [1], which becomes Boussinesq model. The other is the so-called "multispeed thermal model," where particle velocities that have different speeds are used. Multispeed thermal model is intended to correctly represent heat characteristics and compressibility. The recipe for constructing the multispeed thermal model has been presented in Ref. [2]. Several authors [3,4] have given a systematic description of how to formulate multispeed LBM thermal models. The study [5] also has presented how to obtain thermohydrodynamics at various levels of accuracy via multispeed LBM. Some models [6–8] have been proposed. However, most of them do not give satisfactory accuracy when applied to numerical simulations. We carefully investigated whether a correct multispeed LBM Bhatnagar-Gross-Krook (BGK) thermal model is possible and how to construct it.

II. CONDITIONS LEADING TO FLUID EQUATIONS

Below are the conditions for the local equilibrium distribution function $f_{ki}^{(0)}$ of the multispeed BGK thermal model for the particle velocity $\mathbf{c}_{ki}$ to lead to fluid equations [2]. The symbol ρ is the density, u_α is the velocity, and e is the internal energy. The subscript symbol k indicates a group of the particle velocities whose speed is c_k, and i indicates the particle velocity's direction. The subscript symbols α, β, and γ indicate the x, y, or z component. D is the space dimension:

$$\sum_k \sum_i f_{ki}^{(0)} = \rho, \tag{1}$$

$$\sum_k \sum_i f_{ki}^{(0)} c_{ki\alpha} = \rho u_\alpha, \tag{2}$$

$$\sum_k \sum_i f_{ki}^{(0)} c_{ki\alpha} c_{ki\beta} = \frac{2}{D}\rho e \delta_{\alpha\beta} + \rho u_\alpha u_\beta, \tag{3}$$

$$\sum_k \sum_i f_{ki}^{(0)} c_{ki\alpha} c_{ki\beta} c_{ki\gamma} = \frac{2}{D}\rho e (u_\alpha \delta_{\beta\gamma} + u_\beta \delta_{\gamma\alpha} + u_\gamma \delta_{\alpha\beta}) + \rho u_\alpha u_\beta u_\gamma, \tag{4}$$

$$\sum_k \sum_i f_{ki}^{(0)} c_k^2 = \rho(2e + u^2), \tag{5}$$

$$\sum_k \sum_i f_{ki}^{(0)} c_k^2 c_{ki\alpha} = \rho u_\alpha \left[\frac{2(D+2)}{D} e + u^2 \right], \tag{6}$$

$$\sum_k \sum_i f_{ki}^{(0)} c_k^2 c_{ki\alpha} c_{ki\beta} = \frac{2}{D}\rho e \left[\frac{2(D+2)}{D} e + u^2 \right] \delta_{\alpha\beta} + \rho u_\alpha u_\beta \left[\frac{2(D+4)}{D} e + u^2 \right]. \tag{7}$$

Equations (1)–(3), (5) and (6) are for a nondissipative (Euler) fluid. Equations (4) and (7) are the requirements for proper dissipative terms in the momentum and energy equations. However, since the conditions (5) and (6) can be derived by contraction from Eqs. (3) and (4), respectively, independent conditions are Eqs. (1)–(4) and (7).

As Eq. (7) contains up to the fourth order of flow velocity u, the local equilibrium distribution function should retain up to the fourth order terms of flow velocity. Consequently, the local equilibrium distribution function is to contain the fourth rank tensor. The left-hand side of Eq. (4) contains the third rank tensor plus the fourth rank tensor in the $f_{ki}^{(0)}$: totally

*Electronic address: watari.minoru@jaxa.jp

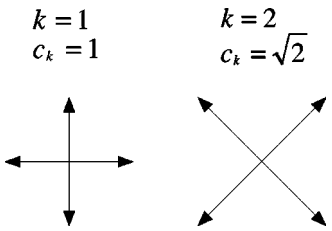

FIG. 1. Basic particle velocities used in the square lattice.

contains up to the seventh rank tensor. As a result, the tensors up to seventh rank should be isotropic.

In the LBM, the particle velocities exactly link the lattice nodes in unit time. Therefore, regular lattice is used: square or hexagonal lattice is used in two dimensions and cubic lattice is used in three dimensions. However, the hexagonal lattice ensures only up to the fifth rank isotropy, which is insufficient to derive the correct fluid equations.

The basic particle velocities used in the square lattice and in the cubic lattice are shown in Fig. 1 and 2, respectively. The odd rank tensors for these particle velocities vanish: isotropic in regard to the odd rank. The even rank tensors generally have the following forms [9]:

$$\sum_i 1 = \pi_k, \tag{8}$$

$$\sum_i c_{ki\alpha} c_{ki\beta} = \chi_k \delta_{\alpha\beta}, \tag{9}$$

$$\sum_i c_{ki\alpha} c_{ki\beta} c_{ki\gamma} c_{ki\xi} = \varphi_k \Delta^{(4)}_{\alpha\beta\gamma\xi} + \psi_k \delta_{\alpha\beta\gamma\xi}, \tag{10}$$

$$\sum_i c_{ki\alpha} c_{ki\beta} c_{ki\gamma} c_{ki\xi} c_{ki\eta} c_{ki\zeta} = \theta_k \Delta^{(6)}_{\alpha\beta\gamma\xi\eta\zeta} + \omega_k \Delta^{(4,2)}_{\alpha\beta\gamma\xi\eta\zeta} + \lambda_k \delta_{\alpha\beta\gamma\xi\eta\zeta}, \tag{11}$$

$$\sum_i c_k^2 c_{ki\alpha} c_{ki\beta} c_{ki\gamma} c_{ki\xi} c_{ki\eta} c_{ki\zeta} = \Theta_k \Delta^{(6)}_{\alpha\beta\gamma\xi\eta\zeta} + \Omega_k \Delta^{(4,2)}_{\alpha\beta\gamma\xi\eta\zeta} + \Lambda_k \delta_{\alpha\beta\gamma\xi\eta\zeta}. \tag{12}$$

The tensors that appear in the above equations are defined as follows:

$$\delta_{\alpha\beta} = 1 \quad (\text{if } \alpha = \beta), = 0 \quad (\text{otherwise}), \tag{13a}$$

$$\delta_{\alpha\beta\gamma\xi} = 1 \quad (\text{if } \alpha = \beta = \gamma = \xi), = 0 \quad (\text{otherwise}), \tag{13b}$$

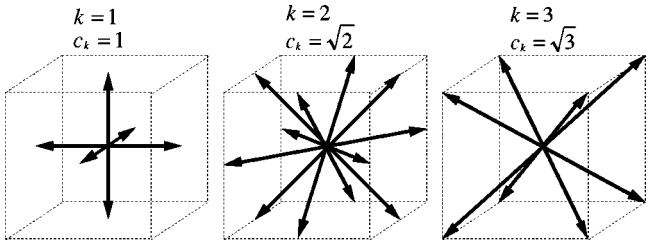

FIG. 2. Basic particle velocities used in the cubic lattice.

TABLE I. Specific values of π_k, χ_k, φ_k, ψ_k, θ_k, ω_k, λ_k, Θ_k, Ω_k, and Λ_k for the basic particle velocities in Fig. 1.

Group	Parameter	$k=1$	$k=2$
c_k^0	π_k	4	4
c_k^2	χ_k	2	4
c_k^4	φ_k	0	4
	ψ_k	2	−8
c_k^6	θ_k	0	4/3
	ω_k	0	0
	λ_k	2	−16
c_k^8	Θ_k	0	8/3
	Ω_k	0	0
	Λ_k	2	−32

$$\delta_{\alpha\beta\gamma\xi\eta\zeta} = 1 \quad (\text{if } \alpha = \beta = \gamma = \xi = \eta = \zeta), = 0 \quad (\text{otherwise}) \tag{13c}$$

$$\Delta^{(4)}_{\alpha\beta\gamma\xi} = \delta_{\alpha\beta}\delta_{\gamma\xi} + \delta_{\alpha\gamma}\delta_{\beta\xi} + \delta_{\alpha\xi}\delta_{\beta\gamma}, \tag{13d}$$

$$\Delta^{(6)}_{\alpha\beta\gamma\xi\eta\zeta} = \delta_{\alpha\beta}\Delta^{(4)}_{\gamma\xi\eta\zeta} + \delta_{\alpha\gamma}\Delta^{(4)}_{\beta\xi\eta\zeta} + \delta_{\alpha\xi}\Delta^{(4)}_{\beta\gamma\eta\zeta} + \delta_{\alpha\eta}\Delta^{(4)}_{\beta\gamma\xi\zeta} + \delta_{\alpha\zeta}\Delta^{(4)}_{\beta\gamma\xi\eta}, \tag{13e}$$

$$\begin{aligned}\Delta^{(4,2)}_{\alpha\beta\gamma\xi\eta\zeta} = {} & \delta_{\alpha\beta}\delta_{\gamma\xi\eta\zeta} + \delta_{\alpha\gamma}\delta_{\beta\xi\eta\zeta} + \delta_{\alpha\xi}\delta_{\beta\gamma\eta\zeta} + \delta_{\alpha\eta}\delta_{\beta\gamma\xi\zeta} \\ & + \delta_{\alpha\zeta}\delta_{\beta\gamma\xi\eta} + \delta_{\beta\gamma}\delta_{\alpha\xi\eta\zeta} + \delta_{\beta\xi}\delta_{\alpha\gamma\eta\zeta} + \delta_{\beta\eta}\delta_{\alpha\gamma\xi\zeta} \\ & + \delta_{\beta\zeta}\delta_{\alpha\gamma\xi\eta} + \delta_{\gamma\xi}\delta_{\alpha\beta\eta\zeta} + \delta_{\gamma\eta}\delta_{\alpha\beta\xi\zeta} + \delta_{\gamma\zeta}\delta_{\alpha\beta\xi\eta} \\ & + \delta_{\xi\eta}\delta_{\alpha\beta\gamma\zeta} + \delta_{\xi\zeta}\delta_{\alpha\beta\gamma\eta} + \delta_{\eta\zeta}\delta_{\alpha\beta\gamma\xi}.\end{aligned} \tag{13f}$$

The tensors $\delta_{\alpha\beta}$, $\Delta^{(4)}_{\alpha\beta\gamma\xi}$, and $\Delta^{(6)}_{\alpha\beta\gamma\xi\eta\zeta}$ are isotropic, whereas, the tensors $\delta_{\alpha\beta\gamma\xi}$, $\delta_{\alpha\beta\gamma\xi\eta\zeta}$, and $\Delta^{(4,2)}_{\alpha\beta\gamma\xi\eta\zeta}$ are anisotropic. The specific values of parameters: π_k, χ_k, φ_k, ψ_k, θ_k, ω_k, λ_k, Θ_k, Ω_k, and Λ_k for the basic particle velocities in Fig. 1 and 2 are listed in Table I and II, respectively. They are grouped into groups c_k^n depending on the influence of particle speed c_k. Note that, if the speeds of particle velocities are doubled, the values of parameters increase to 2^n times of the basic values.

III. MODEL DERIVATION

There seem to be two ways to define the local equilibrium distribution function. One is to distribute weighting coefficients on the whole expansion equation. The other is to distribute weighting coefficients to each power term of the expansion equation. Both models are discussed.

A. Deriving a model that has global coefficients

This type of local equilibrium distribution function was adopted by H. Chen *et al.* [3] and Takada *et al.* [8]. The local equilibrium distribution function that retains up to the fourth

TABLE II. Specific values of π_k, χ_k, φ_k, ψ_k, θ_k, ω_k, λ_k, Θ_k, Ω_k, and Λ_k for the basic particle velocities in Fig. 2.

Group	Parameter	$k=1$	$k=2$	$k=3$
c_k^0	π_k	6	12	8
c_k^2	χ_k	2	8	8
c_k^4	φ_k	0	4	8
	ψ_k	2	−4	−16
c_k^6	θ_k	0	0	8
	ω_k	0	4	−16
	λ_k	2	−52	128
c_k^8	Θ_k	0	0	24
	Ω_k	0	8	−48
	Λ_k	2	−104	384

order of flow velocity is defined as follows. It is derived by expanding the Maxwellian distribution regarding flow velocity. Weighting coefficients F_k are placed on the whole polynomial,

$$f_{ki}^{(0)} = \rho F_k \left[\left(1 - \frac{D}{4e}u^2 + \frac{D^2}{32e^2}u^4 \right) + \frac{D}{2e}\left(1 - \frac{D}{4e}u^2 \right) c_{ki\alpha}u_\alpha + \frac{D^2}{8e^2}\left(1 - \frac{D}{4e}u^2 \right) c_{ki\alpha}c_{ki\beta}u_\alpha u_\beta + \frac{D^3}{48e^3}c_{ki\alpha}c_{ki\beta}c_{ki\gamma}u_\alpha u_\beta u_\gamma + \frac{D^4}{384e^4}c_{ki\alpha}c_{ki\beta}c_{ki\gamma}c_{ki\xi}u_\alpha u_\beta u_\gamma u_\xi \right]. \tag{14}$$

This local equilibrium distribution function is applied to conditions (1)–(4) and (7). Considering that the odd rank tensors vanish and the even rank tensors are expressed by Eqs. (8)–(12), equations to determine coefficients F_k are derived. They are summarized in Table III.

Let us discuss a two-dimensional model ($D=2$). Since ω_k and Ω_k are zeros for both $k=1$ and $k=2$ in Table I, the equations $\Sigma\omega_k F_k=0$ and $\Sigma\Omega_k F_k=0$ are removed from the requirements for F_k. Therefore, to satisfy eight independent constraints, eight speeds of particle velocities are necessary. A model using a rest particle and seven groups of moving particles (four speeds of basic particles $k=1$ and three speeds of basic particles $k=2$), as shown in Fig. 3, was constructed. The coefficients F_k are determined by solving the following equations:

$$\begin{bmatrix} 1 & 4 & 4\times 2^0 & 4\times 3^0 & 4\times 4^0 & 4 & 4\times 2^0 & 4\times 3^0 \\ 0 & 2 & 2\times 2^2 & 2\times 3^2 & 2\times 4^2 & 4 & 4\times 2^2 & 4\times 3^2 \\ 0 & 0 & 0\times 2^4 & 0\times 3^4 & 0\times 4^4 & 4 & 4\times 2^4 & 4\times 3^4 \\ 0 & 2 & 2\times 2^4 & 2\times 3^4 & 2\times 4^4 & -8 & -8\times 2^4 & -8\times 3^4 \\ 0 & 0 & 0\times 2^6 & 0\times 3^6 & 0\times 4^6 & 4/3 & 4/3\times 2^6 & 4/3\times 3^6 \\ 0 & 2 & 2\times 2^6 & 2\times 3^6 & 2\times 4^6 & -16 & -16\times 2^6 & -16\times 3^6 \\ 0 & 0 & 0\times 2^8 & 0\times 3^8 & 0\times 4^8 & 8/3 & 8/3\times 2^8 & 8/3\times 3^8 \\ 0 & 2 & 2\times 2^8 & 2\times 3^8 & 2\times 4^8 & -32 & -32\times 2^8 & -32\times 3^8 \end{bmatrix} \begin{bmatrix} F_0 \\ F_{11} \\ F_{12} \\ F_{13} \\ F_{14} \\ F_{21} \\ F_{22} \\ F_{23} \end{bmatrix} = \begin{bmatrix} 1 \\ e \\ e^2 \\ 0 \\ e^3 \\ 0 \\ 8e^4 \\ 0 \end{bmatrix}. \tag{15}$$

The results for coefficients F_k are shown in Table IV.

For a three-dimensional model ($D=3$), there are ten independent constraints. Ten speeds of particle velocities are necessary. A model using a rest particle and nine groups of moving particles (four speeds of basic particles $k=1$, three speeds of basic particles $k=2$, and two speeds of basic particles $k=3$), was constructed. The results for coefficients F_k are shown in Table V.

B. Deriving a model that has distributed coefficients

This type of local equilibrium distribution function is used by Alexander *et al.* [6] and Y. Chen *et al.* [7]. The distribution function has weighting coefficients: A_k, M_k, G_k, J_k, Q_k, H_k, S_k, R_k, and T_k, on each power term,

$$f_{ki}^{(0)} = \rho(A_k + M_k c_{ki\alpha}u_\alpha + G_k u^2 + J_k c_{ki\alpha}c_{ki\beta}u_\alpha u_\beta + Q_k c_{ki\alpha}u_\alpha u^2 + H_k c_{ki\alpha}c_{ki\beta}c_{ki\gamma}u_\alpha u_\beta u_\gamma + S_k u^4 + R_k c_{ki\alpha}c_{ki\beta}u_\alpha u_\beta u^2 + T_k c_{ki\alpha}c_{ki\beta}c_{ki\gamma}c_{ki\xi}u_\alpha u_\beta u_\gamma u_\xi). \tag{16}$$

This local equilibrium distribution function is applied to conditions (1)–(4) and (7). Considering tensor expressions (8)–(12), equations to determine weighting coefficients are derived and are summarized in Table VI.

The numbers of independent constraints for weighting coefficients of the two-dimensional model are summarized in Table VII. The highest number of independent constraints is four for J_k and R_k. Therefore, four different speeds are necessary. Consequently, one-degree arbitrariness exists in determining the coefficients A_k, M_k, G_k, Q_k, H_k, and S_k. Trivial solution $T_k=0$ can be chosen because the right-hand sides of

TABLE III. Equations for the coefficients F_k for the global coefficient model.

Group	Equations
c_k^0	$\sum_k \pi_k F_k = 1$
c_k^2	$\sum_k \chi_k F_k = \frac{2}{D} e$
c_k^4	$\sum_k \varphi_k F_k = \frac{4}{D^2} e^2$
	$\sum_k \psi_k F_k = 0$
c_k^6	$\sum_k \theta_k F_k = \frac{8}{D^3} e^3$
	$\sum_k \omega_k F_k = 0$
	$\sum_k \lambda_k F_k = 0$
c_k^8	$\sum_k \Theta_k F_k = \frac{16(D+6)}{D^4} e^4$
	$\sum_k \Omega_k F_k = 0$
	$\sum_k \Lambda_k F_k = 0$

the T_k equations are all zero. This analysis exactly coincides with the discussion of Ref. [7].

Same procedure will be developed for the three-dimensional model. Unfortunately there is a mistake in three-dimensional parameters of Table I of Ref. [7]: ($\Theta_{11}=0$, $\Theta_{21}=8$, $\Theta_{31}=0$) should be ($\Theta_{11}=0$, $\Theta_{21}=0$, $\Theta_{31}=8$). Therefore, their three-dimensional model of 3D40V in Table III of Ref. [7] does not give correct solutions. Actually, we confirmed it by Couette simulations.

IV. VERIFICATION OF THE PROPOSED MODELS

Thermal models were evaluated by numerical simulations. The simulations were conducted by applying the Euler and the second upwind finite difference scheme to the following differential equation:

$$\frac{\partial f_{ki}}{\partial t} + c_{ki\alpha}\frac{\partial f_{ki}}{\partial r_\alpha} = -\frac{1}{\phi}(f_{ki} - f_{ki}^{(0)}), \tag{17}$$

where f_{ki} is the distribution function for the particle velocity $\mathbf{c}_{ki}$, t is time, r_α is the spatial coordinate, and ϕ is the relaxation parameter.

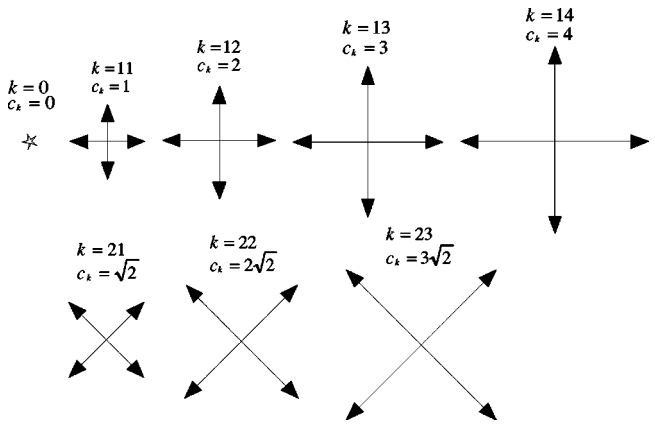

FIG. 3. Particle velocities used in the two-dimensional model proposed in this paper.

The viscous coefficient μ, the thermal conductivity κ', and the pressure P are given as the following equations:

$$\mu = \frac{2}{D}\rho e \phi, \tag{18}$$

$$\kappa' = \frac{2(D+2)}{D^2}\rho e \phi, \tag{19}$$

$$P = \frac{2}{D}\rho e. \tag{20}$$

The ratio of specific heats γ and the speed of sound c are expressed as

$$\gamma = \frac{D+2}{D}, \tag{21}$$

$$c = \sqrt{\gamma \frac{2}{D} e}. \tag{22}$$

TABLE IV. Weighting coefficients for the two-dimensional global coefficient model.

Coefficient	Value
F_0	$1-4(F_{11}+F_{12}+F_{13}+F_{14})$ $-4(F_{21}+F_{22}+F_{23})$
F_{11}	$(-24e^4+85e^3-106e^2+48e)/60$
F_{12}	$(24e^4-80e^3+89e^2-24e)/240$
F_{13}	$(-264e^4+735e^3-574e^2+144e)/11\,340$
F_{14}	$(36e^4-70e^3+49e^2-12e)/13\,440$
F_{21}	$(4e^4-13e^3+12e^2)/32$
F_{22}	$(-4e^4+10e^3-3e^2)/320$
F_{23}	$(12e^4-15e^3+4e^2)/12\,960$

TABLE V. Weighting coefficients for the three-dimensional global coefficient model.

Coefficient	Value
F_0	$1-6(F_{11}+F_{12}+F_{13}+F_{14})$ $-12(F_{21}+F_{22}+F_{23})$ $-8(F_{31}+F_{32})$
F_{11}	$(-3878e^4+1495e^3-19026e^2+9072e)/17\,010$
F_{12}	$(518e^4-2295e^3+3366e^2-1296e)/19\,440$
F_{13}	$(-778e^4+3045e^3-3486e^2+1296e)/153\,090$
F_{14}	$(148e^4-420e^3+441e^2-162e)/272\,160$
F_{21}	$(24e^4-71e^3+54e^2)/324$
F_{22}	$(-42e^4+125e^3-54e^2)/12\,960$
F_{23}	$(8e^4-15e^3+6e^2)/43\,740$
F_{31}	$(-2e^4+4e^3)/81$
F_{32}	$(2e^4-e^3)/5184$

A. Couette flow

Heat characteristics were verified. The upper wall, which is H apart from the lower wall and has internal energy e_2, starts to move at speed U. The lower wall has e_1 and is at rest. Theoretical internal energy distribution e along vertical axis y in a steady state is given as

$$e = e_1 + (e_2 - e_1)\frac{y}{H} + \frac{\mu}{2\kappa'}U^2\frac{y}{H}\left(1-\frac{y}{H}\right). \tag{23}$$

As the value $\mu/2\kappa'$ is constant (=0.25 for the two-dimensional model and =0.3 for the three-dimensional model), the distribution does not depend on the relaxation parameter ϕ. Figure 4 shows the simulation results of the proposed two-dimensional model for various relaxation parameters. The result agrees completely with the theoretical prediction.

Same simulations were conducted using the two-dimensional models of Ref. [6,7]. The result for the model of Ref. [6] is shown in Fig. 5. The result shows dependence on ϕ, which contradicts the theoretical prediction. We think this contradiction is caused from their model that retains up to the third order of flow velocity in the equilibrium distribution function and ensures the isotropy only up to the fifth rank. The result for the model of Ref. [7], which is shown in Fig. 6, also shows dependence on ϕ, though it is less.

B. Evolution from circularly distributed temperature

The isotropic diffusivity of the proposed two-dimensional model was verified. Initially, the internal energy inside the radius r_1 has a higher value e_2 than the value e_1 of the rest of the region. The density is set as the pressure is kept uniform P_1 over the whole region. As the boundary condition, the

TABLE VI. Equations for the coefficients A_k, M_k, G_k, J_k, Q_k, H_k, S_k, R_k, and T_k for the distributed coefficient model.

Coefficients	Group	Equations
A_k	c_k^0	$\sum_k \pi_k A_k = 1$
	c_k^2	$\sum_k \chi_k A_k = \frac{2}{D}e$
	c_k^4	$\sum_k [(D+2)\varphi_k + \psi_k]A_k = \frac{4(D+2)}{D^2}e^2$
M_k	c_k^2	$\sum_k \chi_k M_k = 1$
	c_k^4	$\sum_k \varphi_k M_k = \frac{2}{D}e$
		$\sum_k \psi_k M_k = 0$
G_k	c_k^0	$\sum_k \pi_k G_k = -\sum_k \chi_k J_k$
	c_k^2	$\sum_k \chi_k G_k = -\frac{1}{2}$
	c_k^4	$\sum_k [(D+2)\varphi_k + \psi_k]G_k = -\frac{D+2}{D}e$
J_k	c_k^4	$\sum_k \varphi_k J_k = \frac{1}{2}$
		$\sum_k \psi_k J_k = 0$
	c_k^6	$\sum_k [(D+4)\theta_k + 2\omega_k]J_k = \frac{D+4}{D}e$
		$\sum_k [(D+8)\omega_k + \lambda_k]J_k = 0$
Q_k	c_k^2	$\sum_k \chi_k Q_k = -3\sum_k \varphi_k H_k$
	c_k^4	$\sum_k \varphi_k Q_k = -\frac{1}{2}$
		$\sum_k \psi_k Q_k = 0$

TABLE VI. (*Continued.*)

Coefficients	Group	Equations
H_k	c_k^4	$\sum_k \psi_k H_k = 0$
	c_k^6	$\sum_k \theta_k H_k = \frac{1}{6}$
		$\sum_k \omega_k H_k = 0$
		$\sum_k \lambda_k H_k = 0$
S_k	c_k^0	$\sum_k \pi_k S_k = -\sum_k \chi_k R_k - 3\sum_k \varphi_k T_k$
	c_k^2	$\sum_k \chi_k S_k = -\sum_k \varphi_k R_k - 3\sum_k \theta_k T_k$
	c_k^4	$\sum_k [(D+2)\varphi_k + \psi_k] S_k$
		$= -\sum_k [(D+4)\theta_k + 2\omega_k] R_k - 3\sum_k \Theta_k T_k$
R_k	c_k^4	$\sum_k \varphi_k R_k = -6\sum_k \theta_k T_k$
		$\sum_k \psi_k R_k = 0$
	c_k^6	$\sum_k [(D+4)\theta_k + 2\omega_k] R_k = -6\sum_k \Theta_k T_k + \frac{1}{2}$
		$\sum_k [(D+8)\omega_k + \lambda_k] R_k = 0$
T_k	c_k^4	$\sum_k \psi_k T_k = 0$
	c_k^6	$\sum_k \omega_k T_k = 0$
		$\sum_k \lambda_k T_k = 0$
	c_k^8	$\sum_k \Omega_k T_k = 0$
		$\sum_k \Lambda_k T_k = 0$

TABLE VII. Numbers of independent constraints for weighting coefficients of the two-dimensional distributed coefficient model.

Coefficient	Number of constraints
A_k	3
M_k	3
G_k	3
J_k	4
Q_k	3
H_k	3
S_k	3
R_k	4
T_k	3

internal energy and the pressure maintain their initial values outside the radius r_2. Figure 7 shows a result of contour lines of the internal energy at some later time. Figure 8 is the distribution of the internal energy at various times. In the figure, corresponding Navier-Stokes solutions are also shown. These figures clearly demonstrate the spatial isotropy and the accurate diffusivity of the model.

C. Recovery from a random fluctuation

To demonstrate the numerical stability of the proposed two-dimensional model, this simulation was conducted. Initially, the internal energy at each node of 50×50 is randomly given in the range of 0.8–1.2. The initial density is given as

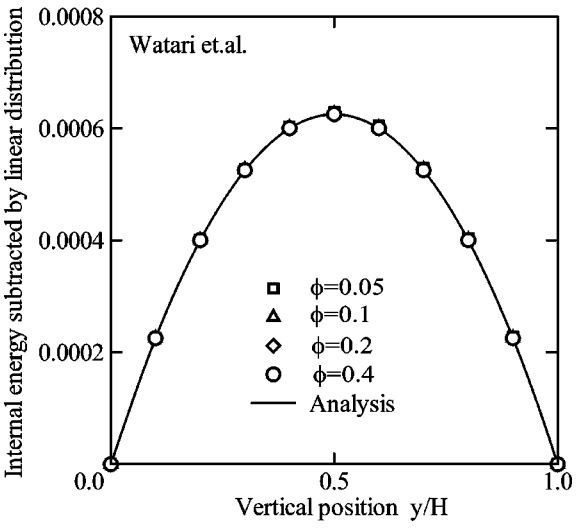

FIG. 4. Couette flow result for the two-dimensional model proposed in this paper. Internal energy distribution at steady state for $U=0.1$ and $e_1=e_2=1.0$. The internal energy subtracted by linear distribution, the last term in Eq. (23), is shown. The relaxation parameter is changed: $\phi=0.05$, 0.1, 0.2, 0.4. The results for all ϕ overlap each other.

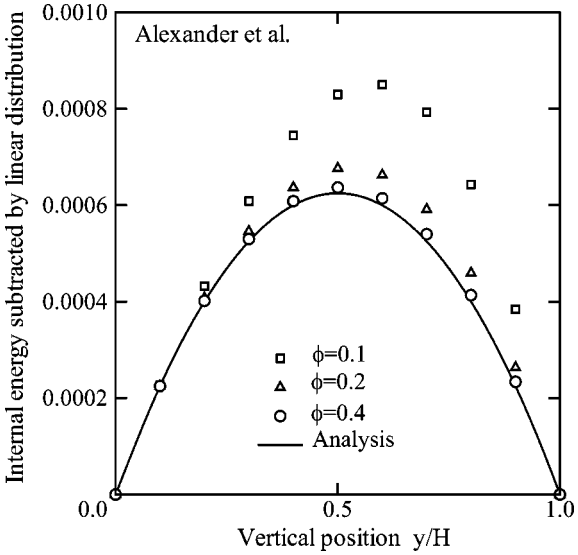

FIG. 5. Couette flow result for the model of Ref. [6]. Internal energy distribution at steady state for $U=0.1$ and $e_1=e_2=0.5$. The relaxation parameter is changed: $\phi=0.1$, 0.2, 0.4. The result shows dependence on ϕ, which contradicts the analytical prediction.

the pressure is kept uniform. Figure 9 shows an example of the evolution of the internal energy distribution. Timewise variations of the internal energy variance for various relaxation parameters are calculated and are shown in Fig. 10. The results show that the fluctuation decays stably to a homogeneous state. In the finite difference LBM scheme, numerical stability can be secured by adjusting time increment. As the relaxation parameter becomes smaller, smaller time increment is needed.

D. Normal shock wave

Compressibility was confirmed by normal shock simulation. The results were compared with theoretical values [10].

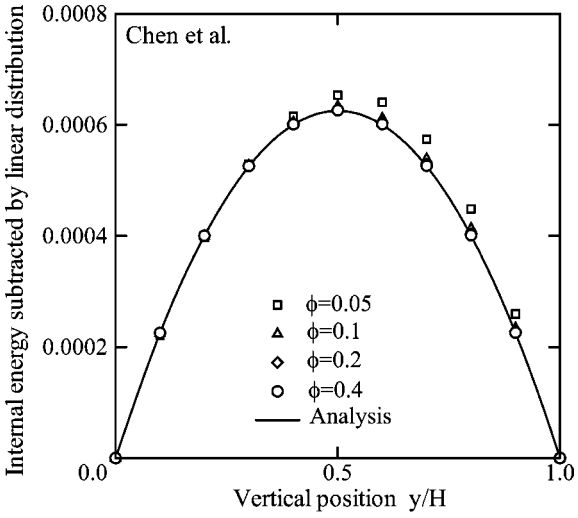

FIG. 6. Couette flow result for the model of Ref. [7]. Internal energy distribution at steady state for $U=0.1$ and $e_1=e_2=0.5$. The relaxation parameter is changed: $\phi=0.05$, 0.1, 0.2, 0.4. Although the model has been improved from the model of Ref. [6], the result still shows dependence on ϕ.

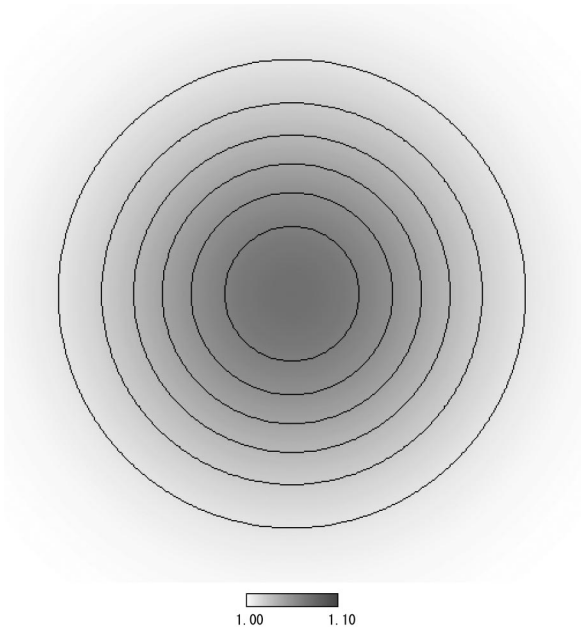

FIG. 7. Evolution from circularly distributed temperature for $r_1=2$, $r_2=7.6$, $e_1=1.0$, $e_2=1.1$, $P_1=1.0$, and $\phi=0.1$. The contour lines of the internal energy: $e=1.01$, 1.02, 1.03, 1.04, 1.05, and 1.06 at $t=7$.

The ratios of flow parameters between upstream and downstream (suffixed by 1 and 2, respectively) of the shock for various upstream Mach numbers were compared with the Rankine-Hugoniot relations in a perfect gas. The result is shown in Fig. 11. The result exactly agrees with the theory.

When the shock is weak, the pressure variation along x axis, normal to the shock, is expressed as the following:

$$P=\frac{1}{2}(P_2+P_1)+\frac{1}{2}(P_2-P_1)\tanh\frac{x}{\delta}, \tag{24}$$

where the origin of position x is taken at $P=\frac{1}{2}(P_2+P_1)$. The shock structure obtained in the simulation for $M_1=1.02$ and $\phi=0.01$ is shown in Fig. 12.

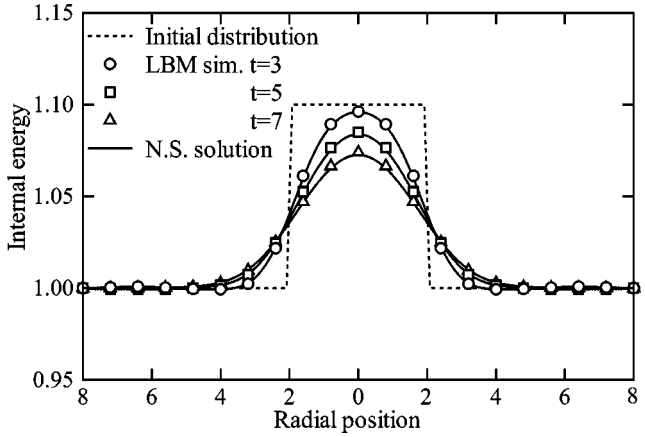

FIG. 8. Evolution from circularly distributed temperature for the same condition as Fig. 7. The internal energy distribution at $t=3$, 5, and 7.

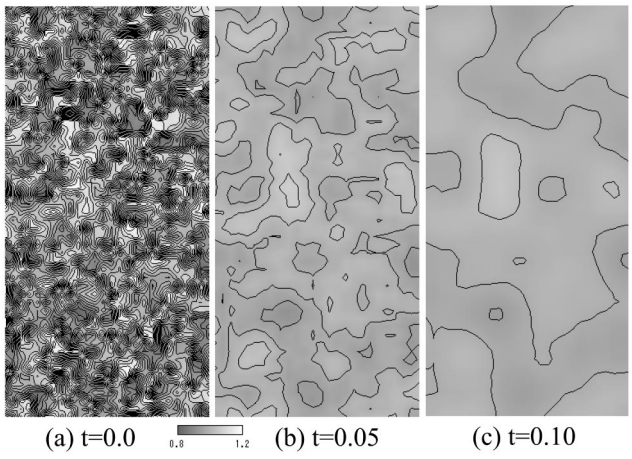

FIG. 9. Recovery from a random fluctuation for $\phi=0.01$. Half regions of internal energy distribution at (a) $t=0.0$, (b) $t=0.05$, and (c) $t=0.1$ are shown.

The thickness of shock δ for monatomic perfect gas with BGK assumption is

$$\delta = \frac{8aV}{(P_2 - P_1)(\partial^2 V/\partial P^2)_s} = \frac{4c}{(P_2 - P_1)(\gamma+1)}\mu\left[\left(2 - \frac{2}{D}\right) + (\gamma - 1)\right], \qquad (25)$$

where V is the specific volume $(=1/\rho)$ and a is the sonic absorption parameter. The thickness δ for various relaxation parameters is shown in Fig. 13. These results exactly agree with the theory.

E. Three-dimensional model

The proposed three-dimensional model was also verified by simulations of Couette flow and normal shock wave. The

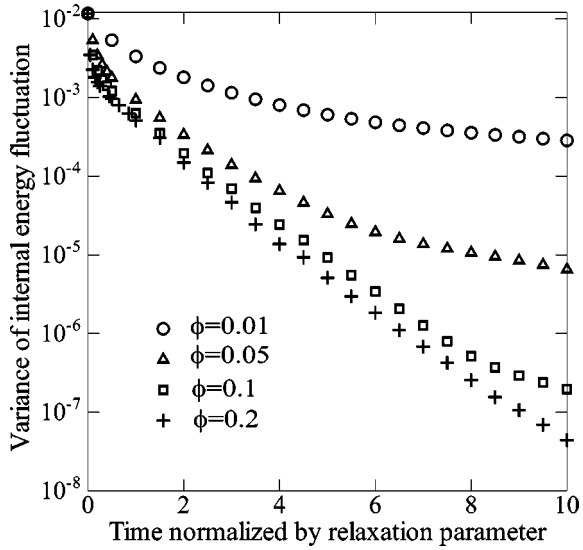

FIG. 10. Recovery from a random fluctuation. The timewise variances of the internal energy fluctuations for various relaxation parameters: $\phi=0.01$, 0.05, 0.1, 0.2.

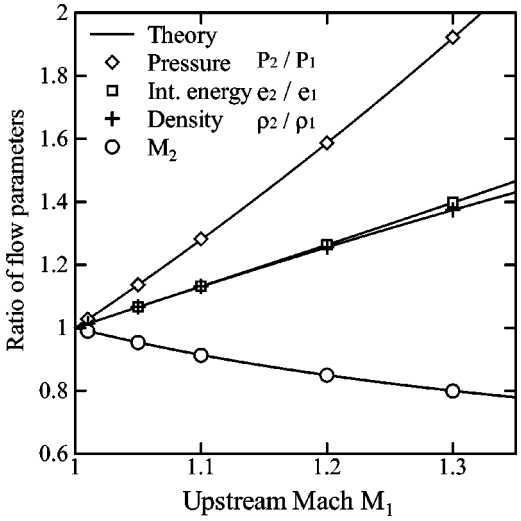

FIG. 11. Ratios of flow parameters between upstream and downstream of the shock for $\phi=0.002$ and various upstream Mach numbers.

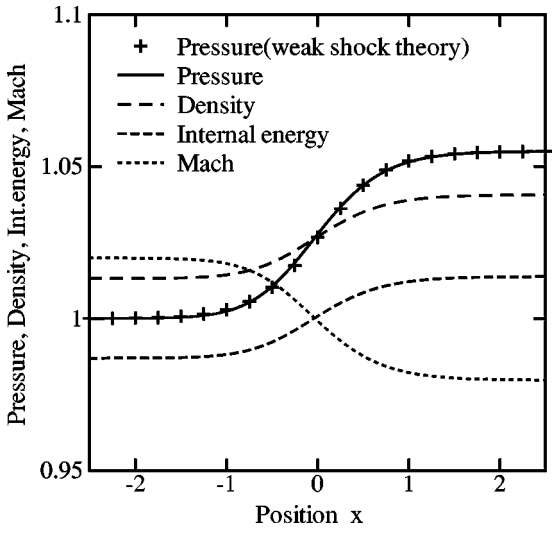

FIG. 12. Normal shock structure for $M_1=1.02$ and $\phi=0.01$.

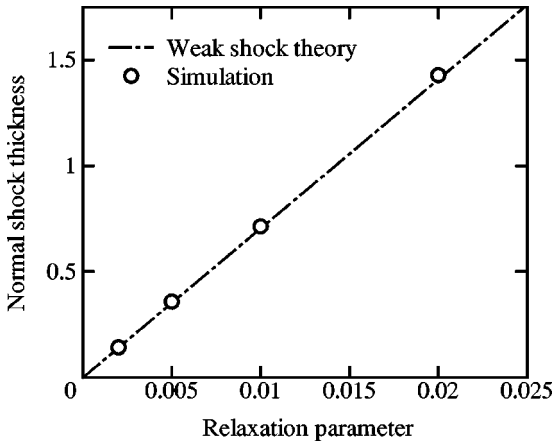

FIG. 13. Thickness of normal shock for $M_1=1.02$. The relaxation parameter is changed: $\phi=0.002$, 0.005, 0.01, 0.02.

model demonstrated the complete accuracy and stability as did the two-dimensional model.

V. CONCLUSIONS

This paper discussed how to construct a correct thermal model. Thermally correct two-dimensional and three-dimensional LBM multispeed models that have global coefficients in the local equilibrium distribution function were proposed. The models were verified by simulations of Couette flow, evolution from circularly distributed temperature, and normal shock wave. The results showed exact agreement with the theoretical predictions. The numerical stability of the model was demonstrated by simulation of recovery from a random fluctuation.

[1] X. He, S. Chen, and G. Doolen, J. Comput. Phys. **146**, 282 (1998).
[2] G. McNamara and B. Alder, Physica A **194**, 218 (1993).
[3] H. Chen, C. Teixeira, and K. Molvig, Int. J. Mod. Phys. C **8**, 675 (1997).
[4] X. Shan and X. He, Phys. Rev. Lett. **80**, 65 (1998).
[5] C. Teixeira, H. Chen, and D. M. Freed, Comput. Phys. Commun. **129**, 207 (2000).
[6] F. J. Alexander, S. Chen, and J. D. Sterling, Phys. Rev. E **47**, R2249 (1993).
[7] Y. Chen, H. Ohashi, and M. Akiyama, Phys. Rev. E **50**, 2776 (1994).
[8] N. Takada, Y. Yamakoshi, and M. Tsutahara, Trans. Jpn. Soc. Mech. Eng., Ser. B **64**, 628 (1998).
[9] S. Wolfram, J. Stat. Phys. **45**, 471 (1986).
[10] L. D. Landau and E. M. Lifshitz, *Fluid Mechanics* (Pergamon, Oxford, 1987).